

## Wearable fluid capture devices for electrochemical sensing of sweat

Guijun Li, Xiaoyong Mo, Wing-Cheung Law and Kang Cheung Chan\*

Advanced Manufacturing Technology Research Centre

Department of Industrial and Systems Engineering

Hong Kong Polytechnic University, Hong Kong

\*E-mail: [kc.chan@polyu.edu.hk](mailto:kc.chan@polyu.edu.hk)

### Abstract

Wearable sensing technologies are vital for realizing personalized health monitoring. Non-invasive human sweat sampling is essential for monitoring an individual's physical state using rich physiological data. However, existing wearable sensing technologies lack the controlled capture of body sweat and in performing on-device measurement without inflammatory contact. Herein, we report the development of a wearable sweat-capture device using patterned graphene arrays with controlled superwettability and electrical conductivity for simultaneously capturing and electrochemically measuring the sweat droplets. The sweat droplets exhibited strong attachment on the superhydrophilic graphene patterns, even during moderate exercising. The captured sweat droplets present strong electrochemical signals using graphene films as the working electrode and metal pins as the counter electrode arrays assembled on 3D printed holders, at the detection limit of 6  $\mu\text{M}$  detection limit for  $\text{H}_2\text{O}_2$  sensing. This research enables full-body spatiotemporal mapping of sweat, beneficial for a broad range of personalized monitoring applications, such as drug abuse detection, athletics performance optimization, and physiological wellness tracking.

**Keywords:** sweat capture, laser scribing, superhydrophobic, electrochemical sensing, graphene

## Introduction

Sweat contains valuable information of inner physiological health.<sup>1</sup> Electrochemical measurement of sweat can enable monitoring of an individual's health at the molecular scale.<sup>2</sup> However, traditional sweat capturing procedures require bulky conductive pads with hard-wired electronic connections in a hospital or laboratory, and are not compatible with frequently monitoring at home.<sup>3</sup> Currently, wearable electronics are booming and facilitate easy biomedical checking of individual's health status, without costly equipment and a team of expensive medical staff. Tiny skin-contact sweat sensors with high electrochemical selectivity have been developed for detecting ions and molecules in sweat, with the capability of transferring the detected physiological signals to smartphones via wireless transmission.<sup>4</sup> However, this skin-contact method is still lacking in robust capturing or storage of sweat in a regulated manner. Colorimetric sensing of sweat with microfluidic guides has also demonstrated high selectivity in detecting lactate, chloride, and glucose with the aid of a smartphone camera. Without a real-time electrical signal, however, this method provides less data than other electrochemical sensing platforms.<sup>5</sup> Although these sweat monitoring methods have demonstrated wearable monitoring capabilities, a better sweat capturing method for electrochemical testing would enable precise, inflammation-free monitoring.

Further, prepatterned superwetting surfaces provide accurate control of fluids on solid surfaces by surface tension, with crucial applications in water harvesting, microfluidics, and liquid separation.<sup>6-9</sup> Surface chemistry and the microstructures collectively determine the wetting properties of solids.<sup>10</sup> With sufficient surface roughness, the superwetting properties of the materials surface can be modified between superhydrophobic and superhydrophilic.<sup>11-12</sup>

For example, by tuning the exposure to UV light, the superwetting properties of  $\text{TiO}_2$  can be significantly changed from superhydrophilic to superhydrophobic.<sup>13</sup> However, the superhydrophobic surfaces gradually changed to superhydrophilic after a certain time, due to the existence of oxygen in the air. Carbon is the most abundant element on earth, and recent research on the wetting properties of graphene have been greatly boosted during the past decade.<sup>14-15</sup> Native graphene, especially in basal plane direction, tends to be hydrophobic,<sup>16</sup> however, pristine graphitic surfaces are more hydrophilic due to the adsorption of hydrocarbons from the air.<sup>17</sup> The traditional graphene synthesis route from wet chemistry usually results in doping on the edges of the graphene flakes, with unreliable wettability. Recently, research on a novel type of graphene, called laser induced graphene from commercial available polyimide, has emerged in fields such as supercapacitors, transducer, and electrocatalysts.<sup>18-21</sup> As the surface wetting property of such graphene films would significantly influence their electrochemical performance, the effect of the gas environment during the laser synthesizing was also carefully studied.<sup>22</sup> Superhydrophilic properties could be maintained within the ambient air and oxygen atmosphere, and superhydrophobic surfaces could be achieved with Ar or  $\text{H}_2$  protection within a chamber. Thus, the oxygen component in the atmosphere would determine the wettability of the graphene films. Although sufficient superhydrophobicity can be achieved with laser scribing under a protecting gas environment, the use of an inert gas chamber greatly limits the potential for mass production. A method capable for fabricating mask-free patterned superhydrophobic and superhydrophilic graphene films in ambient environments is challenging. Recently, we reported a Janus superhydrophobic/superhydrophilic graphene film for solar desalination.<sup>23</sup> Herein, we further develop a two-stage scribing strategy to directly fabricate superhydrophilic and superhydrophobic patterns as wearable sweat capture devices. The graphene patterns can work as work electrodes with strong electrochemical signals for on-device sweat electrolyte sensing.

## Results and Discussion

The fabrication process for the newly developed wearable sweat capture device is illustrated in Figure 1. The yellow polyimide turns to layered graphite (grey square) after the first lower laser scribing (as shown in Figure S1a), and further to porous graphene (black circles) after the second higher laser scribing (as shown in Figure S1b), as illustrated in Figure 1a. From the molecular point of view, the highlighted C=O, C-N, and C-O bonds (Figure 1b) within these polyimide structures are more sensitive to photochemical and thermal influence than the aromatic C-C bonds. After the initial scribing, the layered polyimide structure (Figure 1c) decomposes to layered graphite structures. (Figure 1d). The carbonized hexagon structures remain while the gas phase products (such as CO<sub>2</sub>) will leave the structures (Figure 1e). Due to the attenuation of the polyimide, the absorbed energy at the top of polyimide film is smaller (when laser is scribing upwards). Since graphite with more Basal planes as outside layers (Figure 1f) usually possesses higher hydrophobicity than graphene with more edges exposed (Figure 1g), the black circles arrays have better water attachment than the grey squares.<sup>23-24</sup>

The wetting properties of these laser patterned graphene films were studied using water contact angle analysis. In Figure 2a, the grey square with one-stage laser scribing shows superhydrophobic behavior for a water droplet, with contact angle larger than 150°. Meanwhile, the black circle area, after two-stage laser scribing, behaves superhydrophilically, as shown in Figure 2b. The surface tension of the superhydrophilic and superhydrophobic interface is so strong that it can hold a droplet of volume up to 6 mL using a circular superhydrophilic pattern with a diameter of 30 mm, as shown in Figure 2c. The superwetting patterns can also hold the water droplet steadily on concave and convex surfaces, as shown in Figure 2d and 2e, respectively. The stability of the water droplets on these superwetting films over time was also tested, as shown in Figure 2f to 2k. During the 30 min observations, the profile of the water

droplet remained unchanged, with only a slight decrease of the water droplet size, due to the evaporation effect.

These patterned superwetting graphene substrates can be used as wearable water capture devices. Using the pristine polyimide as the band, the water capture device can be readily integrated into a sweat capture band as shown in Figure 3a. The water droplet shows significant attachment to the superhydrophilic patterns, due to the outside superhydrophobic patterns with confined surface tension. The water droplets can firmly attach to the substrate when facing upwards (Figure 3b), sideways (Figure 3c) and even downwards (Figure 3d). Even during moderate exercise, 96% of the droplets would remain on the substrates, as shown in the video in the supplementary information. Due to its lightweight, flexible and high-scalability nature, this water droplet capture device can be used on the full body (Figure 4a, b), either curved or flat. So it possesses the capability for direct sensing of sweat during exercising, as illustrated in Figure 4c.

The device is also able to directly collect sweat and electrochemically monitor the physiological status on human skin, as it can be directly attached to human skin as in Figure 5a. When a nearby sweat droplet is formed (Figure 5b), the droplet might further move onto the sweat capture device by either gravity or the acceleration force due to the body movement (Figure 5c). After the droplet further moves away from the device, small amounts of sweats will remain on the superhydrophilic patterns (Figure 5d). Then with corresponding metal electrode arrays (Figure 5e), the individual droplet can be electrochemically tested using the conducting graphene and metal electrode as the working and counter electrodes, respectively. Using a 1 mm diameter superhydrophilic pattern, a 3  $\mu\text{L}$  aqueous solution can be held and measured using this two-electrodes setup. The captured NaCl aqueous solutions with concentrations ranging from  $5 \times 10^{-6}$  to  $5 \times 10^{-1}$  M can be easily identified using this setup (Figure S2). The human sweat in an identical volume of 3  $\mu\text{L}$  shows an even stronger signal,

as in Figure S3, measured using this sweat capture device (inset), with similar linear sweep voltammetry behavior as the 1X PBS solution (Figure S4). Thus, this tiny sweat capture device can detect sufficiently strong signal from the collected sweat for characterization using electrochemical sensing.

The glucose is one of the main compositions within the human sweat. With the addition of glucose oxidase modification on graphene electrode,  $\text{H}_2\text{O}_2$  molecules can be generated (Figure 6a).<sup>25</sup> When the  $\text{H}_2\text{O}_2$  molecule reaches the graphene electrode, the reduction of graphene surface would induce a current (Figure 6b), sufficiently large for sensing of the glucose level. The amperometric detection of  $\text{H}_2\text{O}_2$  using graphene as the working electrode was performed at a fixed potential of -0.1 V in 0.1 M PBS solution, as shown in Figure 6c. During the amperometric detection measured with a graphene electrode, a gradually decreased reduction current was recorded with 2  $\mu\text{M}$  concentration step increasing of  $\text{H}_2\text{O}_2$  within the PBS solution. So the superhydrophilic laser induced graphene can directly sense the electrochemical reduction of  $\text{H}_2\text{O}_2$  to  $\text{H}_2\text{O}$ .

The wearable sweat capture device is a vital component among various kinds of wearable electronics. Sweat provides much information about the physiological status of a person, which is important for everyday health monitoring as well as the exercising performance evaluation. The chloride level in the sweat has long been used for evaluating cystic fibrosis.<sup>26-27</sup> The levels of  $\text{Na}^+$  and  $\text{K}^+$  reflect the status of the plasma components within the human body, indicating if people might be suffering from stress.<sup>28</sup> The glucose level in the sweat can also reflect the inner level of glucose, which can non-invasively and continuously reveal diabetes.<sup>29-30</sup> A wearable sweat capture device with electrochemical measuring capability can make the monitoring of these important physiological parameters possible.

The wearable sweat capture device demonstrates capture of sweat as well as the in situ electrochemical testing capabilities. When the sweat droplet flows over the wearable sweat

capture device due to either gravity or the acceleration force during human body movement, the surface tension from the superhydrophilic and superhydrophobic contrasting patterns can collect and store sufficient amounts of sweat on the device. Then subsequent electrochemical measurement can provide high sensitivity characterization for the electrolytes within the sweat droplet. This flexible, lightweight and scalable sweat device can easily adapt to different locations on the human body. The non-contact feature of the droplet to the skin also prevents the potential exposure to side products during the electrochemical testing (such as chlorine). Finally, combining raw materials from commercial polyimide and the compatibilities with the roll-to-roll fabrication process, these sweat capture devices are mass production compatible.

This graphene based sweat capture device also shows great advantage over existing methods. The 200  $\mu\text{m}$  thick device based on polyimide and graphene is light in weight, so it is suitable for wearable electronic applications.<sup>4, 31</sup> The scalability of this method also suits the device for a broad range of ages, from newborn babies, teenagers to adults. The non-contact feature of the test area also permits broad selection of enzymes and other recognition elements on the electrochemical testing areas, without any inflammation issues.<sup>32</sup> The mask-free patterning fabrication process can save time and lower the cost compared to other lithography patterning methods.<sup>33</sup> The synthesized films are naturally flexible while maintaining the water manipulation features, and is more wearable friendly compared to rigid devices. The semiconducting nature of graphene can be directly used as an electrode, without further deposition of noble metals for electrochemical testing.<sup>30</sup> Although superhydrophobicity and superhydrophilicity have been reported using a closed chamber with  $\text{H}_2$  or  $\text{O}_2$  gas, the use of a chamber and additional gas decreases the feasibility for large scale implementation of this method, due to the higher cost and limited spaces of the chamber.<sup>22</sup> Without a size-limiting chamber, our current research for achieving superhydrophilic and superhydrophobic surfaces in ambient environments can be easily fabricated at low cost. So it is more economical and

practical to commercialize this strategy for real applications. In general, this wearable sweat capture device demonstrates great advancement compared to existing technologies.

However, there are still some limitations for the current study. Although the electrochemical tests have already proved the sensing capabilities of the electrolytes, the selectivity of the electrolyte ions is not known. In coming research, different enzymes, reference electrodes and ions filtering components will be added to the individual elements of the probe arrays in Figure 5e for selectively sensing different elements within the captured sweat.<sup>31</sup> The signal to noise ratio of the current graphene is still not satisfying, so some functional materials will be added to graphene patterns for enhancing the H<sub>2</sub>O<sub>2</sub> detection signal in the future work, such as ZnO nanowires and Prussian blue.<sup>34-35</sup> The current electrochemical testing processes are still using the large electrochemical stations of weight over 2 kg, and since the synthesized graphene is electrically conducting, a circuit with these graphene-based conducting lines will be assembled into the device, combining the sweat capture, electrochemical test, and wireless data communication into one single wearable device.<sup>36</sup> In addition, this open system architecture without a microfluidic sealing might face other challenges, such as possibility of containment due to the exposure to environments, and risk of concentration variation because of the evaporation, which are both worthy of further research and development in the near future. With these further studies, a full wearable sweat sensing device will provide a complete solution for sweat based health and performance monitoring.

## Conclusions

A wearable sweat capturing device for electrochemical sensing, based on two-stage laser scribing, is reported. Using commercial polyimide, the device can be made using two stage laser scribing. With the 3D printed electrode arrays, the collected sweat droplets can be



electrochemically analyzed, producing a strong signal even at 3  $\mu\text{L}$  volume. This sweat capturing device is flexible, lightweight and scalable, and can be used at various of locations on the human body. In addition, the electrochemical testing location does not contact the human skin, which provides wider selections of testing materials compared to tight-seal contact devices. This research work has led to a novel solution for wearable sweat capture with high chemical sensing capabilities and is a milestone for practical sweat-sensing based health monitoring.

## **Experimental**

The 200  $\mu\text{m}$  thick polyimide film was used as purchased from Shenzhen Ze Sheng Electronic Company. The carbonized process was performed using a DMG Lasertec 40 Nd: YAG 1064 nm laser at CW mode with scanning rate of 800 mm/s using 3 W power for the initial scribing. After the first-step scribing, the whole polyimide film was converted to black color graphene. Then a second laser scribing was performed with the scanning rate of 800 mm/s using 0.3 W power. The microstructures and their corresponding elementary distributions were characterized using a Tescan MAIA3 Field Emission Scanning Electron Microscope (FESEM) with Energy Dispersive X-ray (EDX) spectroscopy. A Sindatek 100SB optical contact angle meter was used to measure the static contact angle using the sessile drop method. The electrical measurement was carried out using a CHI 660E electrochemical station with a two-electrode configuration. The probe arrays for the electrochemical arrays were designed with Autodesk 3Ds Max and printed with a Makerbot thermoplastic 3D printer, and manually assembled with stainless steel needles.

## **Acknowledgements**

The project was funded by the Postdoctoral Fellowship Scheme of the Hong Kong Polytechnic University with project number G-YW2R.

### Conflict of Interest

The authors declare no conflict of interest.

### Supporting Information

The Supporting information is available free of charge on the ACS Publications websites at DOI:

SEM images of the laser induced graphene with two stage laser scribing, the LSV profile of NaCl, sweat, and PBX solution.

### Reference

1. Heinzerian, P.; Dey, R. D.; Flux, M.; Said, S. I., Deficient Vasoactive Intestinal Peptide Innervation in the Sweat Glands of Cystic-Fibrosis Patients. *Science* **1985**, 229 (4720), 1407-1408.
2. Yang, Y.; Gao, W., Wearable and Flexible Electronics for Continuous Molecular Monitoring. *Chem. Soc. Rev.* **2018**. DOI:10.1039/C7CS00730B
3. Choi, J.; Ghaffari, R.; Baker, L. B.; Rogers, J. A., Skin-Interfaced Systems for Sweat Collection and Analytics. *Sci. Adv.* **2018**, 4 (2), eaar3921.
4. Gao, W.; Emaminejad, S.; Nyein, H. Y. Y.; Challa, S.; Chen, K. V.; Peck, A.; Fahad, H. M.; Ota, H.; Shiraki, H.; Kiriya, D.; Lien, D. H.; Brooks, G. A.; Davis, R. W.; Javey, A., Fully Integrated Wearable Sensor Arrays for Multiplexed in Situ Perspiration Analysis. *Nature* **2016**, 529 (7587), 509-514.
5. Koh, A.; Kang, D.; Xue, Y.; Lee, S.; Pielak, R. M.; Kim, J.; Hwang, T.; Min, S.; Banks, A.; Bastien, P.; Manco, M. C.; Wang, L.; Ammann, K. R.; Jang, K. I.; Won, P.; Han, S.; Ghaffari, R.; Paik, U.; Slepian, M. J.; Balooch, G.; Huang, Y. G.; Rogers, J. A., A Soft, Wearable Microfluidic Device for the Capture, Storage, and Colorimetric Sensing of Sweat. *Sci. Transl. Med.* **2016**, 8 (366), 366ra165.
6. Kim, H.; Yang, S.; Rao, S. R.; Narayanan, S.; Kapustin, E. A.; Furukawa, H.; Umans, A. S.; Yaghi, O. M.; Wang, E. N., Water Harvesting from Air with Metal-Organic Frameworks Powered by Natural Sunlight. *Science* **2017**, 356 (6336), 430-432.
7. Mouterde, T.; Lehoucq, G.; Xavier, S.; Checco, A.; Black, C. T.; Rahman, A.; Midavaine, T.; Clanet, C.; Quere, D., Antifogging Abilities of Model Nanotextures. *Nat. Mater.* **2017**, 16 (6), 658-663.

8. Gupta, D.; Sarker, B.; Thadikaran, K.; John, V.; Maldarelli, C.; John, G., Sacrificial Amphiphiles: Eco-Friendly Chemical Herders as Oil Spill Mitigation Chemicals. *Sci. Adv.* **2015**, *1* (5), e1400265.
9. Ge, J.; Shi, L. A.; Wang, Y. C.; Zhao, H. Y.; Yao, H. B.; Zhu, Y. B.; Zhang, Y.; Zhu, H. W.; Wu, H. A.; Yu, S. H., Joule-Heated Graphene-Wrapped Sponge Enables Fast Clean-up of Viscous Crude-Oil Spill. *Nat. Nanotechnol.* **2017**, *12* (5), 434-440.
10. Genzer, J.; Efimenko, K., Creating Long-Lived Superhydrophobic Polymer Surfaces through Mechanically Assembled Monolayers. *Science* **2000**, *290* (5499), 2130-2133.
11. Chiou, N. R.; Lui, C. M.; Guan, J. J.; Lee, L. J.; Epstein, A. J., Growth and Alignment of Polyaniline Nanofibres with Superhydrophobic, Superhydrophilic and Other Properties. *Nat. Nanotechnol.* **2007**, *2* (6), 354-357.
12. Erbil, H. Y.; Demirel, A. L.; Avci, Y.; Mert, O., Transformation of a Simple Plastic into a Superhydrophobic Surface. *Science* **2003**, *299* (5611), 1377-1380.
13. Feng, X. J.; Zhai, J.; Jiang, L., The Fabrication and Switchable Superhydrophobicity of TiO<sub>2</sub> Nanorod Films. *Angewandte Chemie-International Edition* **2005**, *44* (32), 5115-5118.
14. Gao, Y.; Cao, T. F.; Cellini, F.; Berger, C.; de Heer, W. A.; Tosatti, E.; Riedo, E.; Bongiorno, A., Ultrahard Carbon Film from Epitaxial Two-Layer Graphene. *Nat. Nanotechnol.* **2018**, *13* (2), 133-138.
15. Kim, K. H.; Oh, Y.; Islam, M. F., Graphene Coating Makes Carbon Nanotube Aerogels Superelastic and Resistant to Fatigue. *Nat. Nanotechnol.* **2012**, *7* (9), 562-566.
16. Li, Z. T.; Wang, Y. J.; Kozbial, A.; Shenoy, G.; Zhou, F.; McGinley, R.; Ireland, P.; Morganstein, B.; Kunkel, A.; Surwade, S. P.; Li, L.; Liu, H. T., Effect of Airborne Contaminants on the Wettability of Supported Graphene and Graphite. *Nat. Mater.* **2013**, *12* (10), 925-931.
17. Xu, K.; Heath, J. R., Wetting Contact with What? *Nat. Mater.* **2013**, *12* (10), 872-873.
18. Zhang, J. B.; Zhang, C. H.; Sha, J. W.; Fei, H. L.; Li, Y. L.; Tour, J. M., Efficient Water-Splitting Electrodes Based on Laser-Induced Graphene. *ACS Appl. Mater. Interfaces* **2017**, *9* (32), 26840-26847.
19. Tao, L. Q.; Tian, H.; Liu, Y.; Ju, Z. Y.; Pang, Y.; Chen, Y. Q.; Wang, D. Y.; Tian, X. G.; Yan, J. C.; Deng, N. Q.; Yang, Y.; Ren, T. L., An Intelligent Artificial Throat with Sound-Sensing Ability Based on Laser Induced Graphene. *Nat. Commun.* **2017**, *8*, 14579.
20. Shao, Y.; Li, J.; Li, Y.; Wang, H.; Zhang, Q.; Kaner, R. B., Flexible Quasi-Solid-State Planar Micro-Supercapacitors Based on Cellular Graphene Films. *Materials Horizons* **2017**, (4), 1145-1150.
21. Lamberti, A.; Clerici, F.; Fontana, M.; Scaltrito, L., A Highly Stretchable Supercapacitor Using Laser-Induced Graphene Electrodes onto Elastomeric Substrate. *Adv. Energy Mater.* **2016**, *6* (10), 1600050.
22. Li, Y. L.; Luong, D. X.; Zhang, J. B.; Tarkunde, Y. R.; Kittrell, C.; Sargunraj, F.; Ji, Y. S.; Arnusch, C. J.; Tour, J. M., Laser-Induced Graphene in Controlled Atmospheres: From Superhydrophilic to Superhydrophobic Surfaces. *Adv. Mater.* **2017**, *29* (27), 1700496.
23. Li, G.; Law, W.-C.; Chan, K. C., Floating, Highly Efficient, and Scalable Graphene Membranes for Seawater Desalination Using Solar Energy. *Green Chem.* **2018**, *20*, 3689-3695.
24. Kozbial, A.; Zhou, F.; Li, Z. T.; Liu, H. T.; Li, L., Are Graphitic Surfaces Hydrophobic? *Acc. Chem. Res.* **2016**, *49* (12), 2765-2773.
25. Liao, C. Z.; Zhang, M.; Niu, L. Y.; Zheng, Z. J.; Yan, F., Highly Selective and Sensitive Glucose Sensors Based on Organic Electrochemical Transistors with Graphene-Modified Gate Electrodes. *Journal of Materials Chemistry B* **2013**, *1* (31), 3820-3829.
26. Pankow, S.; Bamberger, C.; Calzolari, D.; Martinez-Bartolome, S.; Lavalley-Adam, M.; Balch, W. E.; Yates, J. R., Delta F508 Cfr Interactome Remodelling Promotes Rescue of Cystic Fibrosis. *Nature* **2015**, *528* (7583), 510-516.

27. Gadsby, D. C.; Vergani, P.; Csanady, L., The Abc Protein Turned Chloride Channel Whose Failure Causes Cystic Fibrosis. *Nature* **2006**, *440* (7083), 477-483.
28. Coppede, N.; Tarabella, G.; Villani, M.; Calestani, D.; Iannotta, S.; Zappettini, A., Human Stress Monitoring through an Organic Cotton-Fiber Biosensor. *Journal of Materials Chemistry B* **2014**, *2* (34), 5620-5626.
29. Lee, H.; Song, C.; Hong, Y. S.; Kim, M. S.; Cho, H. R.; Kang, T.; Shin, K.; Choi, S. H.; Hyeon, T.; Kim, D. H., Wearable/Disposable Sweat-Based Glucose Monitoring Device with Multistage Transdermal Drug Delivery Module. *Sci. Adv.* **2017**, *3* (3), e1601314.
30. Lee, H.; Choi, T. K.; Lee, Y. B.; Cho, H. R.; Ghaffari, R.; Wang, L.; Choi, H. J.; Chung, T. D.; Lu, N. S.; Hyeon, T.; Choi, S. H.; Kim, D. H., A Graphene-Based Electrochemical Device with Thermoresponsive Microneedles for Diabetes Monitoring and Therapy. *Nat. Nanotechnol.* **2016**, *11* (6), 566-572.
31. Emaminejad, S.; Gao, W.; Wu, E.; Davies, Z. A.; Nyein, H. Y. Y.; Challa, S.; Ryan, S. P.; Fahad, H. M.; Chen, K.; Shahpar, Z.; Talebi, S.; Milla, C.; Javey, A.; Davis, R. W., Autonomous Sweat Extraction and Analysis Applied to Cystic Fibrosis and Glucose Monitoring Using a Fully Integrated Wearable Platform. *Proc. Natl. Acad. Sci. U. S. A.* **2017**, *114* (18), 4625-4630.
32. Miyamoto, A.; Lee, S.; Cooray, N. F.; Lee, S.; Mori, M.; Matsuhisa, N.; Jin, H.; Yoda, L.; Yokota, T.; Itoh, A.; Sekino, M.; Kawasaki, H.; Ebihara, T.; Amagai, M.; Someya, T., Inflammation-Free, Gas-Permeable, Lightweight, Stretchable on-Skin Electronics with Nanomeshes. *Nat. Nanotechnol.* **2017**, *12* (9), 907-914.
33. Timonen, J. V. I.; Latikka, M.; Leibler, L.; Ras, R. H. A.; Ikkala, O., Switchable Static and Dynamic Self-Assembly of Magnetic Droplets on Superhydrophobic Surfaces. *Science* **2013**, *341* (6143), 253-257.
34. Han, W. X.; He, H. X.; Zhang, L. L.; Dong, C. Y.; Zeng, H.; Dai, Y. T.; Xing, L. L.; Zhang, Y.; Xue, X. Y., A Self-Powered Wearable Noninvasive Electronic-Skin for Perspiration Analysis Based on Piezo-Biosensing Unit Matrix of Enzyme/Zno Nanoarrays. *ACS Appl. Mater. Interfaces* **2017**, *9* (35), 29526-29537.
35. Karyakin, A. A.; Puganova, E. A.; Budashov, I. A.; Kurochkin, I. N.; Karyakina, E. E.; Levchenko, V. A.; Matveyenko, V. N.; Varfolomeyev, S. D., Prussian Blue Based Nanoelectrode Arrays for H<sub>2</sub>O<sub>2</sub> Detection. *Anal. Chem.* **2004**, *76* (2), 474-478.
36. Liu, S. H.; Fu, Y.; Li, G. J.; Li, L.; Law, H. K. W.; Chen, X. F.; Yan, F., Conjugated Polymer for Voltage-Controlled Release of Molecules. *Adv. Mater.* **2017**, *29* (35), 1701733.

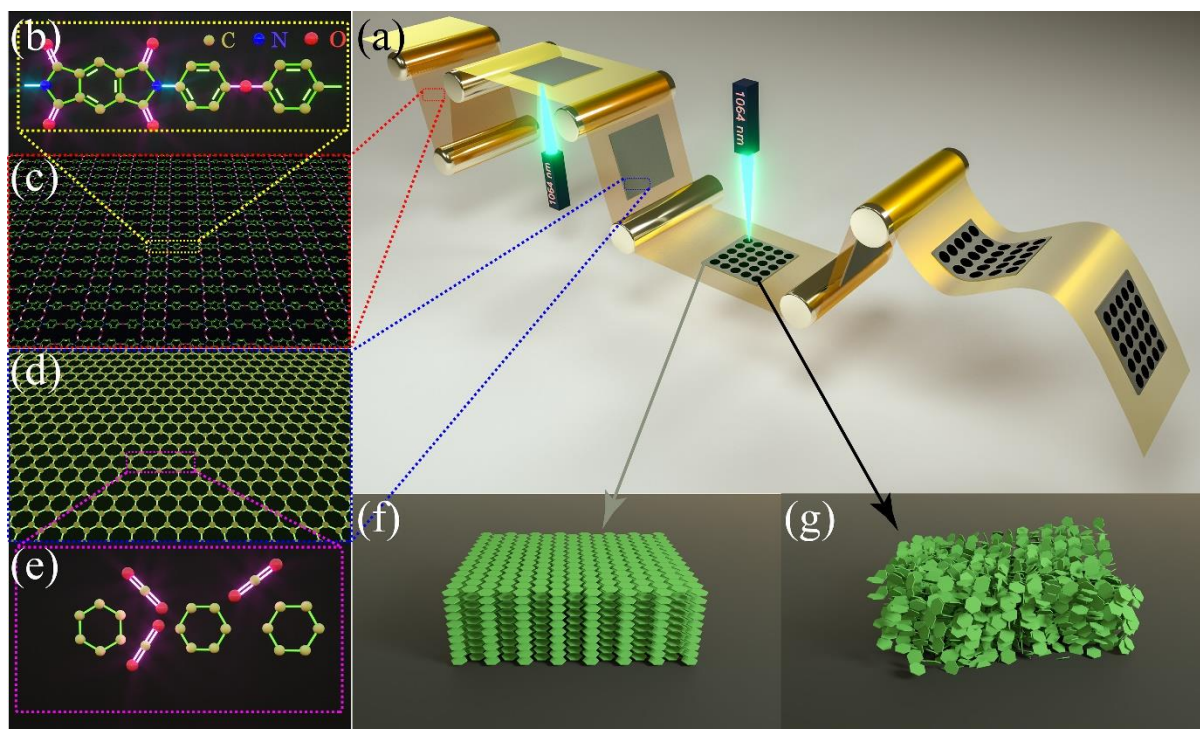


Figure 1 Schematic illustration of the chemical composition and microstructure fabrication process of the wearable sweat capture device. (a) The yellow polyimide film changes to graphite and graphene respectively after the lower and higher laser scribing, respectively. The raw material of the fabrication is polyimide polymer (c), with its (b) dissociation bonds highlighted. The laser scribing carbonizes the polyimide into graphite(d), with an aromatic structure and gas phase  $\text{CO}_2$  (e). The top layer of polyimide after the initial bottom laser scribing (left, bottom) is graphite, as shown by the grey squares and the green layered hexagons(f). The top layer of polyimide after the second laser scribing (top, right) is porous graphene, as shown as the black circles and the random orientated hexagons(g).



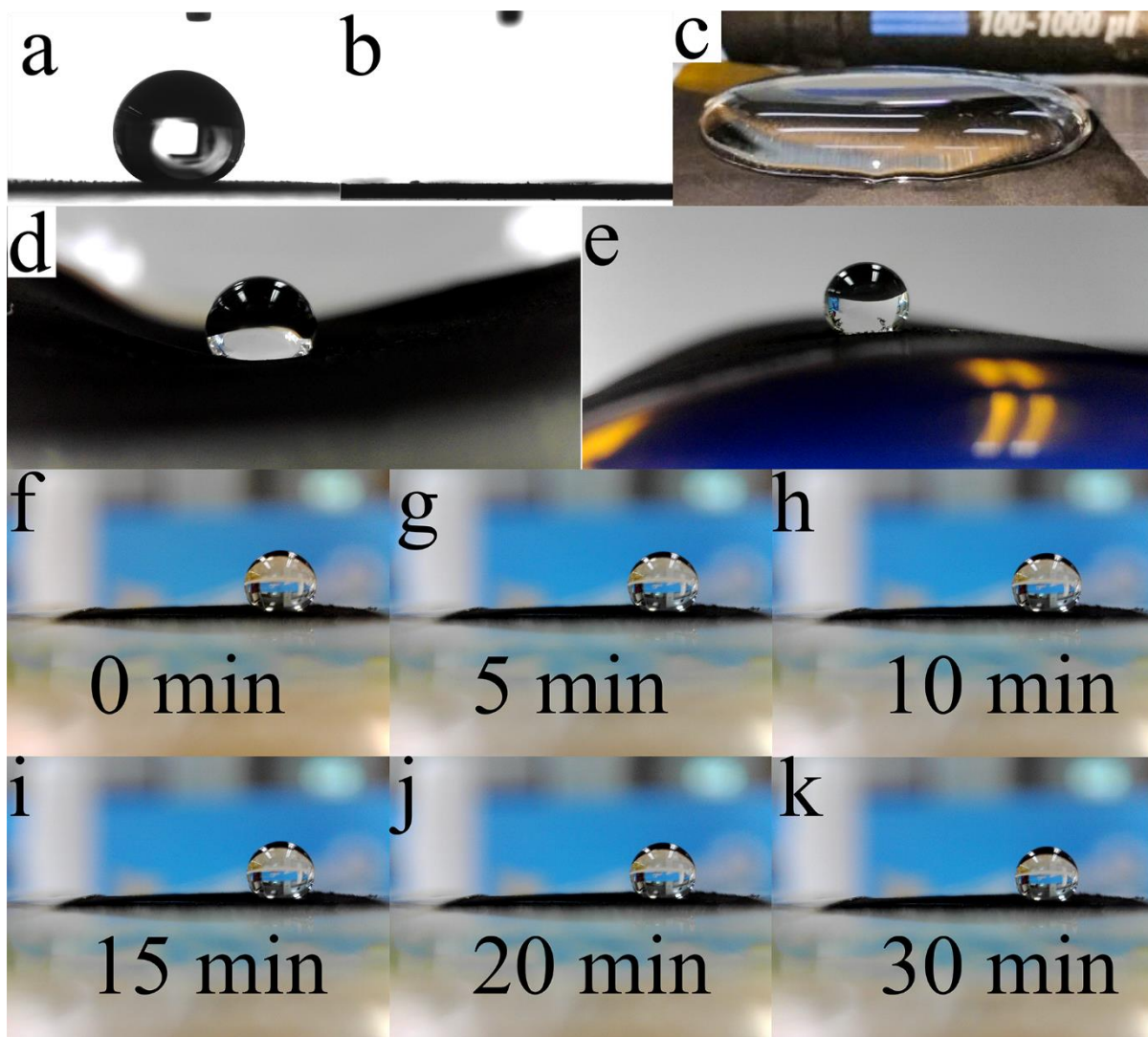


Figure 2 Superwetting properties of the laser induced graphene. (a) Contact angle of the superhydrophobic layer. (b) Contact angle of the superhydrophilic layer. (c) A 30 mm diameter superhydrophilic circle holding a 6 mL droplet. (d) Surface confined droplet holding on the concavely bended film. (e) Surface confined droplet holding on the convexly bended film. (f)-(k) The droplet holding on the superwetting film with different time.



Figure 3 Demonstration of the wearable water-capturing device. (a) A wristband type water capture device worn on the human arm, with captured water when facing up (b), sideways (c), and down (d).



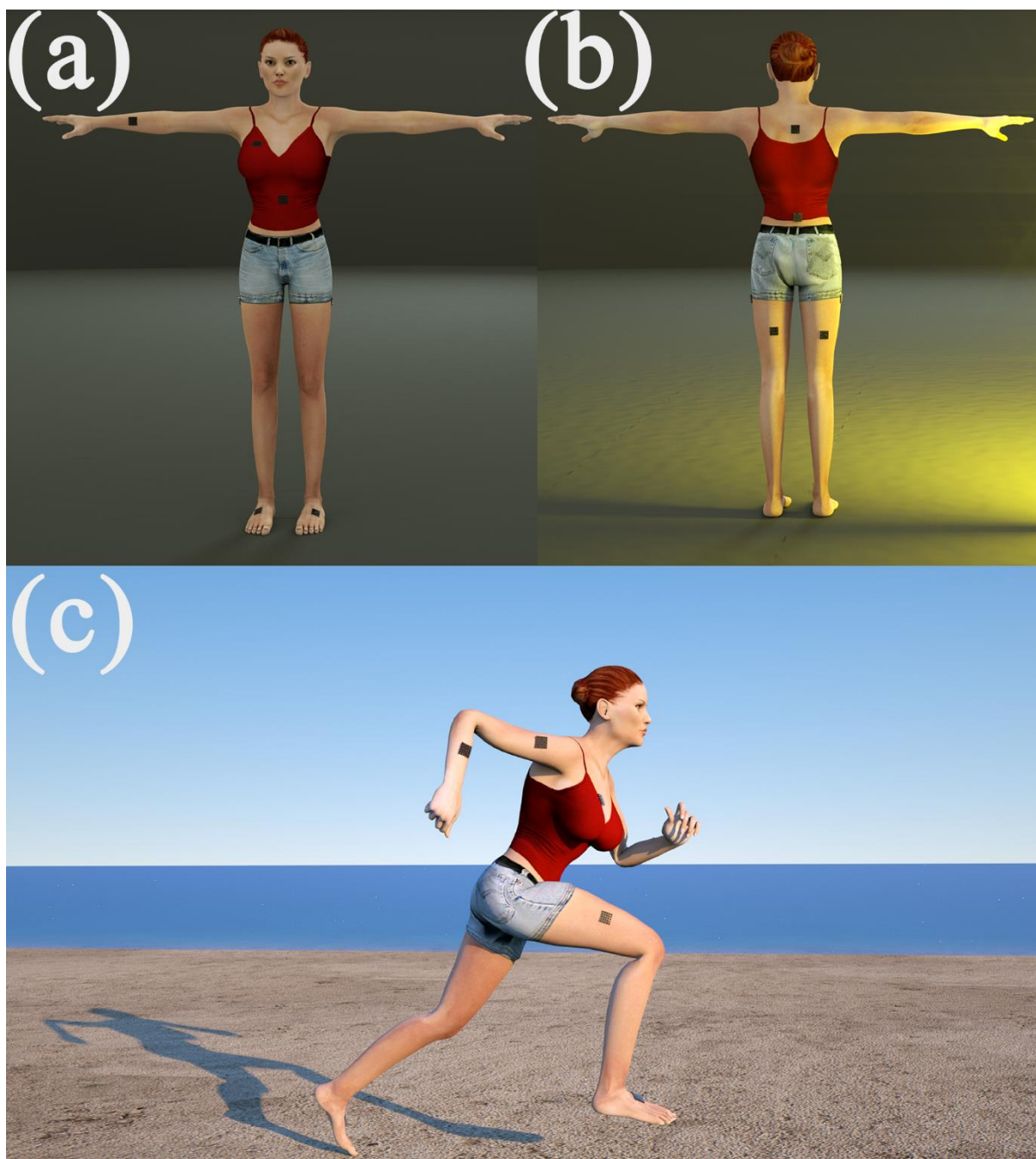


Figure 4 Schematic illustration for using this wearable device for sweat capturing at various locations of human body. (a) Frontal view, (b) back view and (c) During exercise.



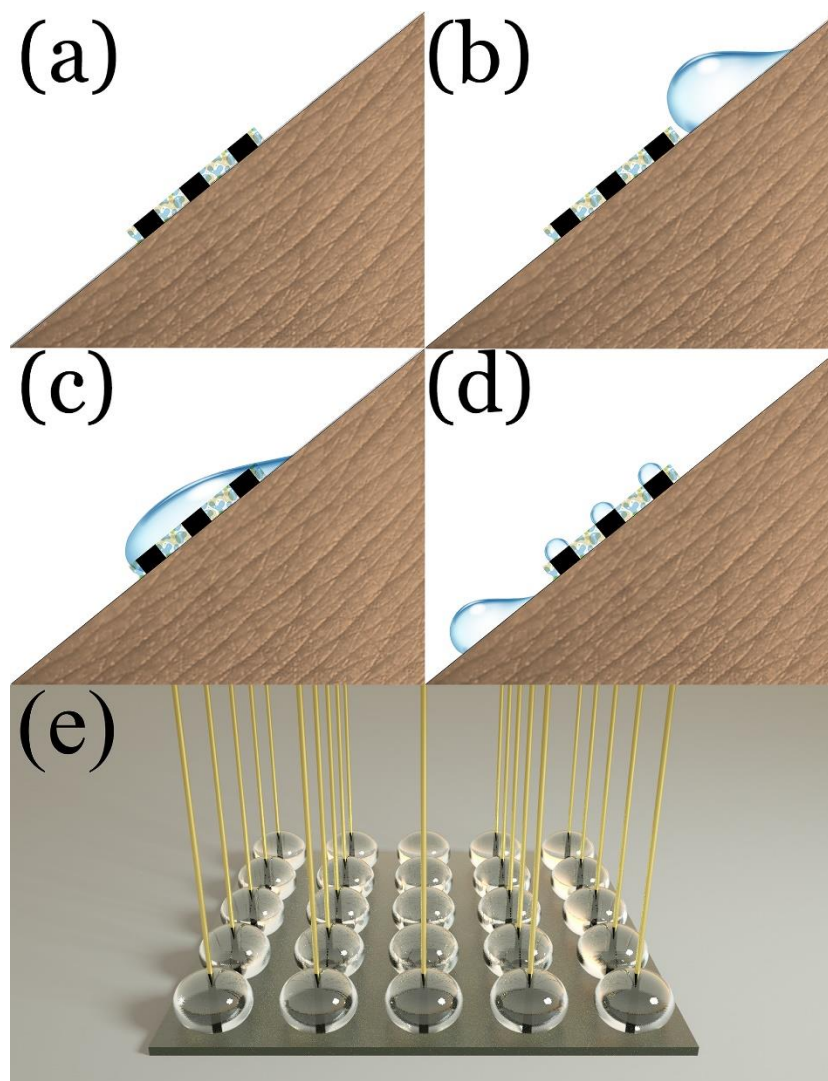


Figure 5 The sweat capture process on skin using this wearable device and their electrochemical test capability. (a) The wearable sweat capture device is place on human skin. (b) When sweat droplet is formatted, it will flow towards the device due to either gravity or acceleration force due to human movement. After the sweat droplet flows over the device(c), a part of the sweat will be captured at the superhydrophilic part of the device (d). (e) Then the metal probe arrays will be attached to the corresponding droplets for electrochemical characterizing the captured sweats.

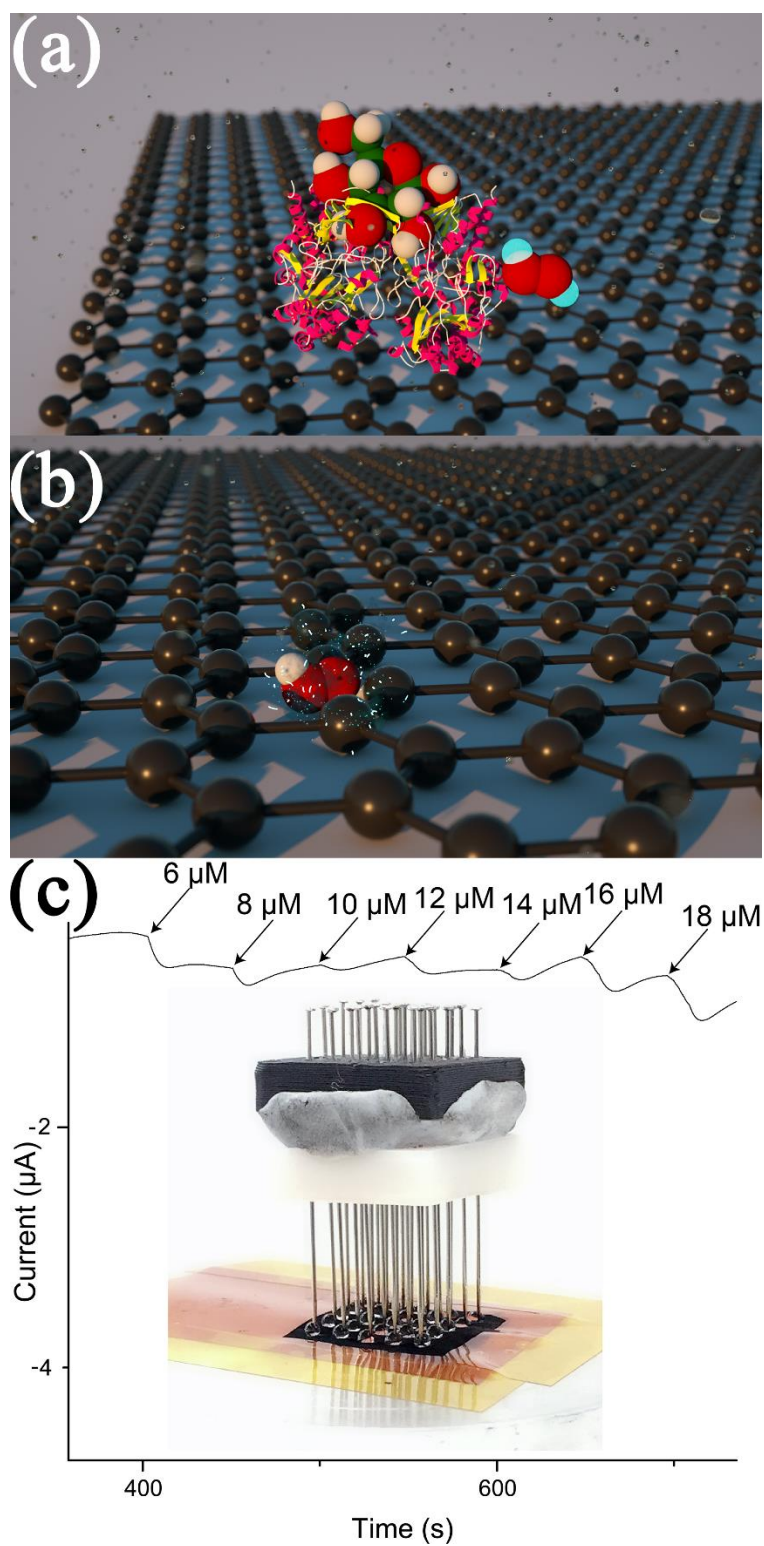


Figure 6 (a) Schematic illustration of glucose within the electrode. (b) schematic illustration of the process of generation of H<sub>2</sub>O<sub>2</sub> due to the glucose oxidase. (c) A current-time response obtained on increasing the H<sub>2</sub>O<sub>2</sub> concentration in 2 μM steps at the graphene electrode with potential fixed at -0.1 V.

## Table of Contents

